Surface Charge Dependence of Polyelectrolyte-Induced Domain Size and Composition in Lipid Bilayer Membranes

Kevin J. Crowell and Peter M. Macdonald*

Department of Chemistry and Erindale College, University of Toronto, 3359 Mississauga Road North, Mississauga, Ontario, Canada L5L 1A2

Received: February 11, 1998; In Final Form: July 22, 1998

^{2}H NMR spectroscopy was used to investigate the response of specifically choline-deuterated 1-palmitoyl-2-oleoyl-*sn*-glycero-3-phosphocholine (POPC) to changes in surface electrostatic charge in lipid bilayer membranes consisting of mixtures of POPC with the anionic lipid 1-palmitoyl-2-oleoyl-*sn*-glycero-3-phosphoglycerol (POPG), plus the cationic polyelectrolyte poly(vinylbenzyltrimethylammonium chloride) (PVTA). The ^{2}H NMR spectra consisted of two overlapping Pake powder patterns, indicating the coexistence of two lipid domains with only slow exchange of lipids between the two. There was no evidence of any nonbilayer lipid arrangements. Analysis of the quadrupolar splittings of the two ^{2}H NMR spectral components for POPC-α-d_2 versus POPC-β-d_2 demonstrated that the two domains differ with respect to their overall surface charge environments and that the PVTA-bound domain was enriched with respect to anionic lipids while the PVTA-free domain was depleted. When the initial bilayer POPG content was varied, the number of POPG molecules associated with each bound PVTA molecule remained constant at a 1:1 POPG anion: PVTA cation equivalents ratio. However, the number of POPC molecules associated with each bound PVTA molecule increased with decreasing initial POPG content. Thus, the surface area occupied per PVTA domain expanded or contracted as the available oppositely charged POPG decreased or increased. This indicates that the PVTA/POPG complex is behaving at the surface like a two-dimensional random-coil polymer undergoing swelling by a solvent, POPC. Within the PVTA-bound domain, the ^{2}H NMR quadrupolar splittings suggest that the PVTA/POPG complex penetrates more deeply into the lipid bilayer than does POPG alone, as might be expected for a neutralized salt pair.

Introduction

Domains in biological membranes have become a topic of considerable interest.[1−7] A membrane domain may be defined as any region having a distinct composition and significant dimension and duration. Two issues of paramount importance concern the physical origin of domains and their biological function. In particular cases such questions can be answered with some certainty. The MARCKS peptide (myristoylated alanine-rich C kinase substrate), for example, contains clusters of basic amino acid residues that laterally segregate acidic phospholipids, like phosphatidylinositol, by virtue of electrostatic attraction.[8] When so segregated the acidic phospholipids cannot participate in the calcium/phospholipid second messenger cell signaling pathway. Upon phosphorylation by protein kinase C, the MARCKS peptide dissociates from the membrane, releasing the segregated phospholipids—a process that has been termed the myristoyl-electrostatic switch.[9] Thus, one function of membrane domains is to manipulate the activity of particular membrane proteins through control of the local environment. Moreover, it is evident that electrostatic attraction is one of the key physical interactions leading to domain formation.

The interactions of basic peptides, such as the MARCKS peptide, with acidic phospholipid-containing lipid bilayers can be modeled quite successfully by combining mass action equations with Gouy−Chapman theory to account for electrostatic accumulation of peptides in the diffuse double layer at the membrane surface.[10] Features such as the sigmoidal dependence of binding on the percentage of acidic phospholipids are reproduced, for example, when it is assumed that each basic residue binds independently to one acidic phospholipid.

Despite this impressive progress, many fundamental aspects of electrostatically induced domain formation have yet to be addressed experimentally. Specifically, the details of domain size and composition, and the effects thereupon of peptide structural variations such as molecular weight, linear charge density and amphiphilicity, or membrane structural variations such as surface charge density and lipid chemistry, are, at best, incompletely understood.

Recently, a new method for detecting electrostatically induced membrane domains has been reported, involving ^{2}H NMR of choline-deuterated 1-palmitoyl-2-oleoyl-*sn*-glycero-3-phosphocholine (POPC).[11−13] On the basis of the well-established "molecular voltmeter" properties of POPC, and the differences in surface electrostatic charge in different membrane domains, the ^{2}H NMR technique has been demonstrated to provide information regarding the composition of individual domains, the global distribution among various domain types, and, with certain qualifications, the domain size.

A convenient model system in which to study electrostatically induced membrane domain formation consists of lipid bilayers in the form of multilamellar vesicles (MLVs) to which one adds synthetic polyelectrolytes. Model membranes such as MLVs allow complete control of bilayer lipid composition and surface charge density, as well as solution pH and osmotic strength.

* Corresponding author. Tel: 905-828-3805. Fax: 905-828-5425. E-mail: pmacdona@credit.erin.utoronto.ca.

10.1021/jp981074o CCC: $15.00
Published on Web 10/17/1998

Using synthetic polyelectrolytes permits one to alter virtually any desired physical or chemical aspect of polyelectrolyte structure, in particular the polymer chain length, degree of branching, linear charge density, or hydrophilic/lipophilic balance.

In this report we describe ^{2}H NMR studies of the effect of lipid bilayer surface charge density on the composition and size of domains induced by the cationic polyelectrolyte PVTA (poly(vinylbenzyltrimethylammonium chloride)) in lipid bilayers composed of mixtures of zwitterionic POPC plus anionic POPG (1-palmitoyl-2-oleoyl-*sn*-glycero-3-phosphoglycerol).

Materials and Methods

Materials. 1-Palmitoyl-2-oleoyl phosphatidic acid (POPA) and nondeuterated POPC and POPG were purchased from Avanti Polar Lipids (Alabaster, AL). Poly(vinylbenzyltrimethylammonium chloride) (PVTA, M_W 40 000, degree of polymerization N 190) was purchased from Polysciences Inc. (Warrington, PA). Tetraphenylboron (TPB) and 2,3,4-triisopropylbenzenesulfonyl chloride (TPS) were purchased from Aldrich (Milwaukee, WI). 4-(2-Hydroxyethyl)piperazine-1-ethanesulfonic acid (HEPES) was purchased from BDH (Toronto, ON).

Synthesis of Choline-Deuterated Phosphatidylcholine. POPC was selectively deuterated at either the α or β positions of the choline headgroup using a strategy based on a combination of the methods of Harbison and Griffin[14] and Aloy and Rabout.[15] In short, POPC-α-d_2 and POPC-β-d_2 were synthesized by coupling the tetraphenylboron salts of the corresponding choline headgroups to POPA, using TPS as the condensing agent.[16] The deuterated phosphatidylcholines were then purified by elution through an Amberlite mixed-bed ion exchanger (BDH, Toronto, ON), followed by acetone precipation, and their purity was determined by thin-layer chromatography (TLC) and by ^{1}H NMR.

Preparation of Multilamellar Vesicles (MLVs). Lipid mixtures of the desired composition were prepared by combining the appropriate volumes of chloroform stock solutions of either POPC-α-d_2 or POPC-β-d_2 and POPG. Typically, 10 mg of the desired deuterated POPC was mixed with the prescribed amount of POPG. The solvent was removed under argon, followed by high vacuum. The dried lipids were then rehydrated in 100−150 μL of 10 mM HEPES, pH 7.4 by gentle warming and vortexing, plus four to seven cycles of freeze−thaw to ensure lipid mixing.

Preparation of MLVs Containing PVTA. The dried lipid mixtures were prepared as described above but were hydrated using 10 mM HEPES (pH 7.4) containing the desired amount of PVTA. Sufficient HEPES buffer was added to bring the final volume to 150 μL. The solution was then gently warmed, vortexed, and subjected to several freeze−thaw cycles to ensure homogeneous mixing.

NMR Measurements. ^{2}H NMR spectra were recorded on a Chemagnetics CMX300 NMR spectrometer operating at 45.98 MHz, using a Chemagnetics wide-line deuterium probe. The quadrupolar echo sequence[17] was employed using quadrature detection with complete phase cycling of the pulse pairs, a 90° pulse length of 1.9 μs, an interpulse delay of 30 μs, a recycle delay of 100 ms, a spectral width of 100 kHz, and a 2K data size. T_2^{qe} for the POPC choline deuterons was measured by recording the spectral intensity as a function of the length of the interpulse delay in the quadrupolar echo pulse sequence.

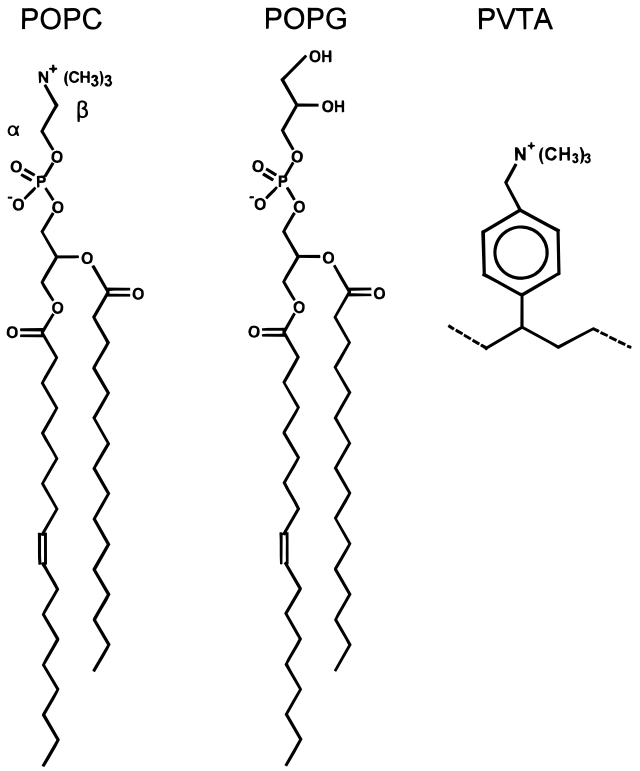

Figure 1. Structures of the zwitterionic phospholipid POPC, the anionic phospholipid POPG, and the monomeric repeat unit of the cationic polyelectrolyte PVTA.

The resulting exponential decay of the spectral intensity was plotted in linear form and the T_2^{qe} was obtained from the slope.

^{31}P NMR spectra were recorded on the same spectrometer operating at 121.25 MHz, using a Chemagnetics double-resonance magic angle spinning (MAS) probe, but without sample spinning. The Hahn echo sequence with complete phase cycling of the pulses and proton decoupling during acquisition was employed as described by Rance and Byrd.[18] The 90° pulse length was 6.5 μs, the echo spacing 40 μs, the recycle delay 2 s, the spectral width 100 kHz, and the data size 2K.

Sample temperature was regulated during acquisition of the NMR spectra using a thermocouple linked to a feedback loop controlling the operation of a resistive heater through which the temperature-regulating air stream stream passed prior to reaching the NMR sample. The sample was always held at the desired temperature for 20 min prior to signal acquisition.

Pake Pattern Spectral Line Shape Simulations. ^{2}H NMR Pake pattern line shapes were simulated using a computer program, written in our laboratory, based on the tiling method introduced by Alderman et al.[19] The simulation variables include the quadrupolar splitting, $\Delta\nu$, the line width parameter, T_2, and the intensity of a given Pake pattern. The program does not include provisions for T_2 asymmetry effects, the lack of which can lead to imperfect simulation of spectral shoulders.

Results and Discussion

^{2}H NMR Evidence for PVTA-Induced Domains in Mixed POPG + POPC Bilayers. Figure 1 shows the structures of the zwitterionic phospholipid POPC, the anionic phospholipid POPG, and the monomeric repeat unit of the cationic polyelectrolyte PVTA. When deuterons are located within the choline headgroup of POPC (deutero-labeling positions are indicated by the α- and β-labeling nomenclature in Figure 1) and POPC

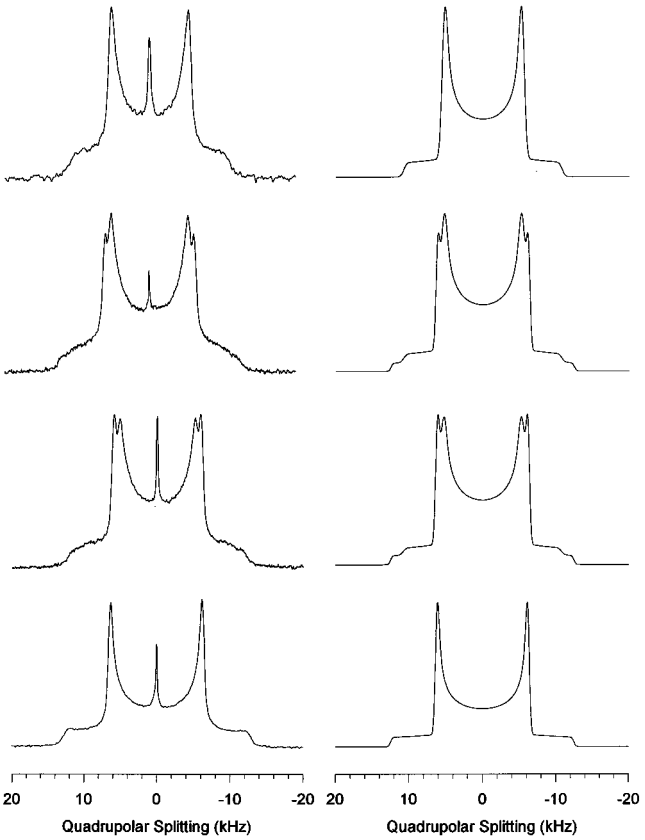

Figure 2. ^{2}H NMR spectra and NMR spectral simulations for mixtures of POPG + POPC-α-d_2 (50/50 M/M) as a function of added PVTA. NMR spectra are shown in the left column, while spectral simulations are shown on the right. The PVTA/POPG ratios are, from top to bottom, 0, 0.33, 0.8, and 1.25. All spectra were acquired at 24 °C.

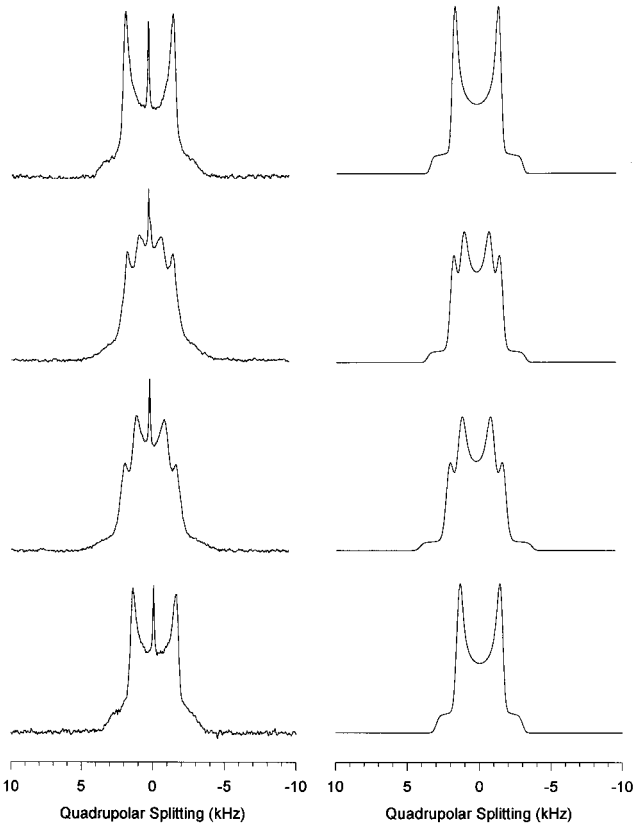

Figure 3. ^{2}H NMR spectra and NMR spectral simulations for mixtures of POPG + POPC-β-d_2 (30/70 M/M) as a function of added PVTA. NMR spectra are shown in the left column, while spectral simulations are shown on the right. The PVTA/POPG ratios are, from top to bottom; 0, 0.4, 0.7, and 1.0. All spectra were acquired at 5 °C.

is assembled into a lipid bilayer membrane, the resulting ^{2}H NMR spectrum consists of a Pake powder pattern,[20,21] examples of which are shown in Figures 2 and 3. From such spectra one measures the quadrupolar splitting, corresponding to the separation, in hertz, between the two spectral maxima or "horns".

A singular aspect of the ^{2}H NMR spectrum of choline-deuterated POPC is that the size of the quadrupolar splitting changes in a characteristic and progressive fashion with changes in the surface charge density of the lipid bilayer. For instance, the top spectrum in Figure 2 was recorded with a mixture of POPG + POPC-α-d_2 (50/50, M/M), yielding a quadrupolar splitting of 10.5 kHz. The top spectrum in Figure 3, on the other hand, was recorded with a mixture of POPG + POPC-β-d_2 (30/70) (all ratios being molar ratios), and the quadrupolar splitting is measured to be 3.1 kHz. With 100% POPC lipid bilayers, by comparison, the quadrupolar splittings are 6.42 kHz for POPC-α-d_2 and 5.80 kHz for POPC-β-d_2. Thus, the negative surface charge produced by mixing in POPG causes the quadrupolar splitting from POPC-α-d_2 to increase while that from POPC-β-d_2 decreases. This inverse response of the quadrupolar splitting from the two POPC choline-deutero-labeling positions to a given surface charge density is characteristic of the so-called "molecular voltmeter" behavior of POPC.[22,23] It is considered to originate with a concerted conformational change undergone by the choline headgroup of POPC as its large dipole moment seeks to align itself with the electrical field emanating outward from the charged lipid bilayer surface. The great utility of this behavior of POPC is that it provides the ability to sense and report on, via ^{2}H NMR, all and any sources of bilayer surface charge, cationic or anionic, whether originating with species intrinsic or extrinsic to the bilayer proper.

When increasing amounts of POPG are mixed into the lipid bilayer, the quadrupolar splitting from POPC-α-d_2 increases progressively while that from POPC-β-d_2 decreases progressively, as shown in Figure 4. Such data constitute a calibration curve from which the POPG concentration experienced by POPC in a particular environment may be deduced using an empirical calibration relation of the form

$$\Delta\nu_i = \Delta\nu_0 + AX_{\mathrm{POPG}} + BX_{\mathrm{POPG}}{}^2 \qquad (1)$$

where $\Delta\nu_i$ is the quadrupolar splitting observed for a given mole fraction of POPG (X_{POPG}) in a particular environment, $\Delta\nu_0$ is the quadrupolar splitting measured for 100% POPC, and A and B are the weighting coefficients listed in Table 1. At low mole fractions of POPG, or over a narrow range of X_{POPG}, the relationship between the quadrupolar splitting and the amount of POPG is approximately linear. Otherwise, X_{POPG} is obtained by solving the quadratic equation for a particular experimental value of $(\Delta\nu_i - \Delta\nu_0)$.

Figure 2 shows a series of ^{2}H NMR spectra obtained at 24 °C with MLVs consisting of mixtures of POPG + POPC-α-d_2 (50/50) to which have been added increasing amounts (from top to bottom) of the cationic polyelectrolyte PVTA. The experimentally obtained spectra on the left are to be compared with the computer-simulated spectra on the right. Upon adding PVTA, a second Pake powder pattern component appears in the ^{2}H NMR spectrum. One spectral component has a quadrupolar splitting larger, and the second a quadrupolar splitting smaller, than that of the control spectrum. With increasing

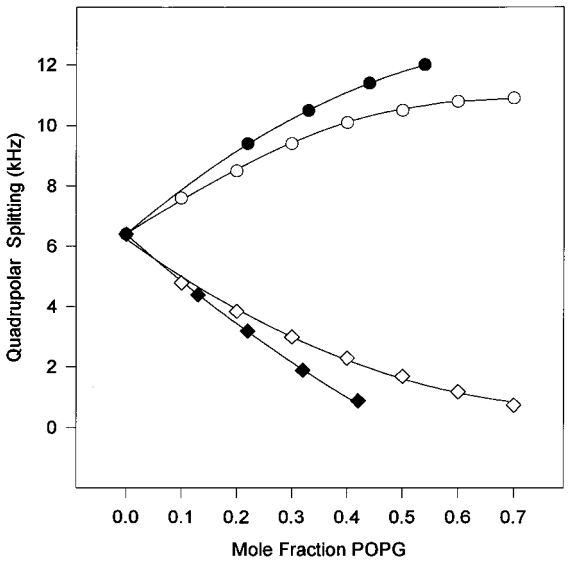

Figure 4. Calibration curves relating the ^{2}H NMR quadrupolar splitting from POPC-α-d_2 (circles) and POPC-β-d_2 (squares) to the mole fraction of POPG. Open symbols represent quadrupolar splittings in the absence of PVTA, while closed symbols represent quadrupolar splittings in environments containing PVTA.

TABLE 1: POPG−POPC Quadrupolar Splitting Calibration Constants[a]

lipid	temp (°C)	$\Delta\nu_0$ (kHz)	A (kHz)	B (kHz)
POPC-α-d_2 + POPG	23	6.42	11.48	−2.26
+ PVTA	23	6.40	15.76	−10.00
POPC-β-d_2 + POPG	23	5.80	−14.07	12.54
	5	6.23	−13.08	7.68
+ PVTA	5	6.40	−16.10	6.58

[a] Quantities correspond to fitted values of coefficients in eq 1 for different deutero-labeling positions and temperatures. PVTA values refer to 1:1 PVTA:POPG complexes as describe in text.

amounts of PVTA the spectral component with the larger quadrupolar splitting grows in intensity at the expense of the other component and eventually dominates the spectrum entirely in the presence of excess PVTA cations relative to POPG anions.

Figure 3 shows a series of ^{2}H NMR spectra obtained at 5 °C with MLVs consisting of mixtures of POPG + POPC-β-d_2 (30/70) to which have been added increasing amounts (from top to bottom) of the cationic polyelectrolyte PVTA. The experimentally obtained spectra on the left are to be compared, again, with the computer-simulated spectra on the right. As was observed with POPC-α-d_2, adding PVTA induces the appearance of a second Pake powder pattern component in the ^{2}H NMR spectrum of POPC-β-d_2. Again, one spectral component has a quadrupolar splitting larger, and the second a quadrupolar splitting smaller, than that of the control spectrum. However, for the case of POPC-β-d_2, the spectral component with the smaller quadrupolar splitting grows in intensity with increasing amounts of PVTA, at the expense of the other component, eventually dominating the spectrum entirely in the presence of excess PVTA.

These ^{2}H NMR results demonstrate that PVTA induces a domain structure in POPG + POPC bilayer membranes, in accord with our previously reported findings on this system.[13] This appears to be a general polyelectrolyte-associated phenomenon, since similar domains are induced in mixed cationic + zwitterionic amphiphile bilayer membranes upon addition of any of a series of different anionic polyelectrolytes.[11,12] The two spectral components correspond to two different environments between which POPC-α-d_2 (or POPC-β-d_2) is distributed, with only slow exchange, on the ^{2}H NMR time scale, between the two. Given the sensitivity of the quadrupolar splitting of choline-deuterated POPC to surface charge effects, and the opposite effects of PVTA on the POPC-α-d_2 versus POPC-β-d_2 quadrupolar splitting, one concludes that the two environments differ primarily with respect to their surface charge densities and that the PVTA-associated domain is enriched with POPG while the PVTA-free domain is correspondingly depleted of POPG.

The ^{2}H NMR spectra indicate, further, that the two environments are remarkably homogeneous in composition. Heterogeneous charge environments would produce a distribution of quadrupolar splittings. Instead, we observe sharp quadrupolar splittings for each environment. The implication is that, for a particular POPG/POPC global ratio and a particular PVTA/POPG equivalence, there is a distinct thermodynamic optimum lipid composition of the PVTA-associated and PVTA-free states.

The ^{2}H NMR spectral simulations shown on the right in each of Figures 2 and 3 consist, generally, of a superposition of two Pake powder components, each of which displays a particular quadrupolar splitting and each of which contributes a particular fractional intensity to the whole. The success of this approach in reproducing the experimentally observed ^{2}H NMR spectra is evident. The utility of these simulations is that they yield the fractional intensity of the two spectral components, which provides, in turn, the proportion of the total POPC-α-d_2 or POPC-β-d_2 population present in the particular bilayer environment.

We note, further, that dePaking of such ^{2}H NMR spectra[24] produces dePaked spectra containing at most two resonances, the quadrupolar splitting of which agree with those measured from the powder spectra (data not shown). Furthermore, the relative integrated areas of the resonances in the dePaked spectra agree within a few percent with the relative intensities of the powder components in the spectral simulations.

In certain cases, where there is only a small difference in the quadrupolar splitting of two spectral components, dePaking the powder spectrum is the best way to extract their respective quadrupolar splitting and intensities. In most cases of interest here, however, our limits of resolution are reached, not when there is an insufficient difference in quadrupolar splitting between two components, but rather when the intensity of a given spectral component becomes too small relative to the other. In such cases, dePaking, with its consequent loss of signal-to-noise, is of little assistance.

In these studies we have not attempted to perform ^{2}H NMR measurements of polyelectrolyte effects on headgroup deuterated POPG. Monovalent lipids, in general, appear to be insensitive to surface electrostatic effects. For instance, the ^{2}H NMR spectrum of headgroup deuterated DMPG changes little as a function of surface charge density.[25] Likewise, headgroup deuterated cationic amphiphiles incorporated into lipid bilayers showed only small changes in their ^{2}H NMR spectra upon addition of polyelectrolyte, and these could be attributed to changes in local orientational order, rather than specific surface charge effects.[26]

PVTA-Induced Domains Contain Phospholipids in a Fluid Bilayer State. Several lines of evidence indicate that the phospholipids within the PVTA-bound domain remain in an essentially fluid bilayer state despite the presence of the polyelectrolyte.

First, successful spectral simulations such as those shown in Figures 2 and 3 are achieved only when it is assumed that both spectral components consist of motionally narrowed Pake

TABLE 2: Effect of PVTA on T_2 Relaxation Times of POPC-α-d_2 or POPC-β-d_2 + POPG Mixtures

POPG/POPC	PVTA/POPG	T_2 (ms)
	POPC-α-d_2	
20/80	0	0.83
	1.50	1.12
40/60	0	0.75
	1.0	1.01
50/50	0	0.82
	1.25	1.27
	POPC-β-d_2	
10/90	0	2.74
	1.5	3.22
30/70	0	1.80
	1.7	2.49
40/60	0	2.59
	1.5	3.43

powder patterns with an asymmetry parameter equal to zero, as expected for fluid lipid bilayers.

Second, dePaking of such experimental spectra (results not shown) always produces dePaked spectra consistent with asymmetry parameters equal to zero.[24]

Third, ^{2}H NMR T_2^{qe} relaxation time measurements on POPC-α-d_2 and POPC-β-d_2 mixed with POPG, with and without PVTA, produce results consistent with fluid phospholipids, as summarized in Table 2. In all such measurements, single-exponential decays of individual spectral components are observed, while T_2^{qe} asymmetry is minimal. As documented in Table 2, it is found that the T_2^{qe} relaxation time of the PVTA-bound spectral component is always longer than that of the PVTA-free spectral component. Regardless, the range of values is compatible with a highly fluid environment for POPC within both the PVTA-bound and PVTA-free domains. No consistent trend in T_2^{qe} is found with respect to the POPG/POPC molar ratio in the lipid bilayers, although T_2^{qe} for POPC-α-d_2 is always shorter than for POPC-β-d_2. We note, further, that in the spectral simulations shown in Figures 2 and 3 the PVTA-bound component always displays a line width parameter smaller than that of the PVTA-free component, consistent with the T_2^{qe} results in Table 2.

As discussed by Köchy and Bayerl,[27] lateral diffusion of phospholipids is expected to be a major contributor to the transverse relaxation of deuterated phospholipids in lipid bilayers. A concise explanation is that lipid lateral diffusion around the radius of curvature of lipid vesicles produces line broadening through the consequent uncertainty in the value of the geometric term $(3\cos^2\theta - 1)$, which dictates the resonance frequency for a particular lipid-attached deuteron, where θ is the angle between the lipid's long molecular axis and the direction of the magnetic field. Our T_2^{qe} observations suggest either that phospholipid lateral diffusion is hindered within the PVTA-bound domains or that the bound PVTA dampens large-scale motions of the lipid ensemble, which would otherwise produce local curvature. 2D ^{2}H NMR exchange spectroscopy would certainly be useful in addressing this question.[27−29]

Fourth, the ^{31}P NMR spectra shown in Figure 5 demonstrate that, even in the presence of excess PVTA, one is dealing with lipids assembled into a bilayer arrangement. The ^{31}P NMR spectra of such mixtures are diagnostic of bilayer versus H_{II} versus isotropic or cubic phases.[30,31] The series of ^{31}P NMR spectra in Figure 5 were obtained with mixtures of POPG + POPC (50/50) plus progressively increasing amounts (from top to bottom) of added PVTA. In the absence of PVTA (top spectrum), the line shape is characteristic of fluid lipids in a bilayer arrangement. The residual chemical shift anisotropy ($\Delta\sigma$ = − 45 ppm) in the spectrum is typical of POPC and/or POPG.[32,33] Of course, this spectrum is a superposition of separate powder contributions from POPC and POPG, which cannot be resolved under these circumstances. With added PVTA, in a ratio of either 0.33 (middle spectrum) or 1.25 (bottom spectrum), PVTA cationic equiv/POPG anionic equiv, there is no change in the macroscopic phase of the lipid bilayer assembly, nor even the appearance of any small component of isotropic lipid. There is, however, a slight increase in the residual chemical shift anisotropy ($\Delta\sigma$ = −53 ppm), as anticipated for the addition of cationic charges.[34] One concludes that the lipid self-assembly maintains an overall planar bilayer architecture upon addition of PVTA.

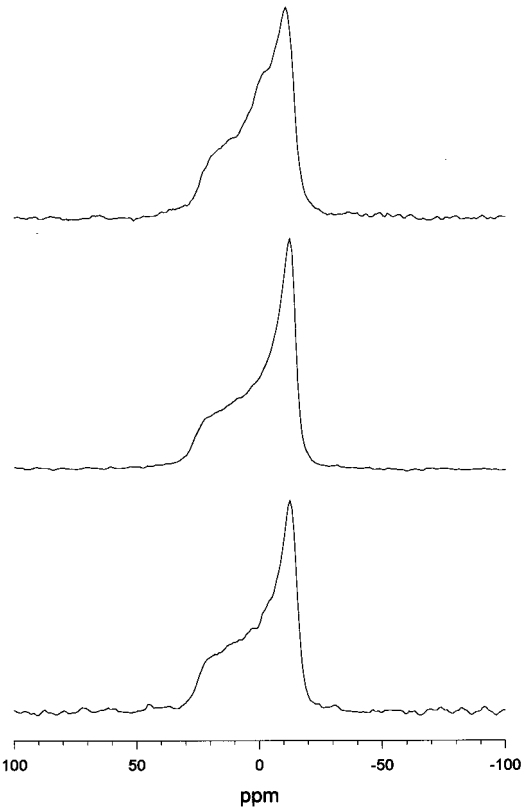

Figure 5. ^{31}P NMR spectra of POPG + POPC-α-d_2 (50/50 M/M) with increasing PVTA/POPG ratios. In the top spectrum the PVTA/POPG ratio is 0, while it is 0.33 and 1.25 for the middle spectrum and lower spectrum, respectively.

We have performed, in addition, ^{31}P MAS NMR measurements on various mixed POPG + POPC lipid bilayers with and without PVTA. Magic angle spinning removes broadening due to chemical shift anistropy like that evident in Figure 5, leaving the isotropic phosphorus resonances of POPG and POPC resolved from one another. We observed no signficant change in either the POPG or POPC isotropic ^{31}P NMR chemical shift upon adding PVTA, nor any evidence of domain structures (data not shown). This simply means that the isotropic chemical shifts of these phospholipids are not very sensitive to surface charge.

Calculating Domain Composition and Size from ^{2}H NMR Spectra. Details of the measured quadrupolar splitting and the intensities of the PVTA-bound and PVTA-free ^{2}H NMR spectral components are shown in Figure 6 for POPC-α-d_2 and in Figure 7 for POPC-β-d_2, as a function of added PVTA and for a range of POPG + POPC mixtures. Note that the values reported for POPC-β-d_2 were all obtained at 5 °C while those reported for POPC-α-d_2 were all obtained at 24 °C. It is generally found that at lower temperatures the resolution of the two spectral

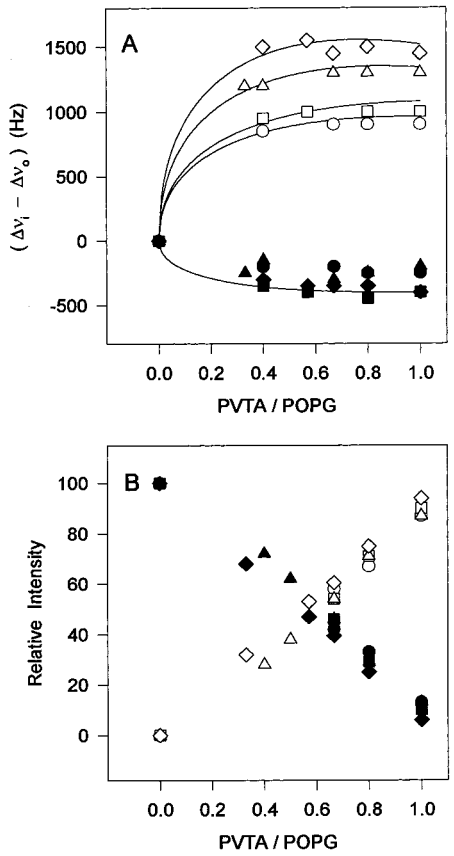

Figure 6. Relative change in the quadrupolar splitting for mixtures of POPG + POPC-α-d_2 (A) and the corresponding intensities of the PVTA-containing and PVTA-free spectral components as obtained from NMR spectral simulations (B). Circles (●) represent 20/80 POPG/POPC mixtures, squares (■) represent 30/70 mixtures, triangles (▲) represent 40/60 mixtures, and diamonds (◆) represent 50/50 mixtures. Closed symbols represent the PVTA-free phase, while open symbols represent the PVTA-bound phase.

components is enhanced but that the enhancement is far more pronounced for POPC-β-d_2 than for POPC-α-d_2 since the temperature dependence of the latter's quadrupolar splitting is rather slight. Resolution of the two spectral components is *the* issue in these measurements. For instance, below a PVTA cation/POPG anion equivalents ratio of about 0.4, resolution of two spectral components is not generally possible, simply because there is as yet insufficient POPC trapped within the PVTA-bound domains.

Figure 6A shows the quadrupolar splitting from both the PVTA-bound and the PVTA-free POPC-α-d_2 spectral components for different molar ratios of POPG present in the original bilayer mixtures, while Figure 6B shows the corresponding intensity changes. The PVTA-bound POPC-α-d_2 is readily identified by the fact that its intensity increases with added PVTA. This spectral component always displays a quadrupolar splitting greater than that of the control. The POPC-α-d_2 within the PVTA-free region always displays a quadrupolar splitting less than that of the control. The implication is that PVTA is able to laterally segregate POPG into a domain enriched with respect to POPG, leaving behind a domain depleted with respect to POPG. One sees that the increase in the quadrupolar splitting of POPC-α-d_2 in the PVTA-bound domain, relative to the controls, is magnified by higher initial POPG levels. For POPC-α-d_2 within the PVTA-free domains, there is a similar, albeit

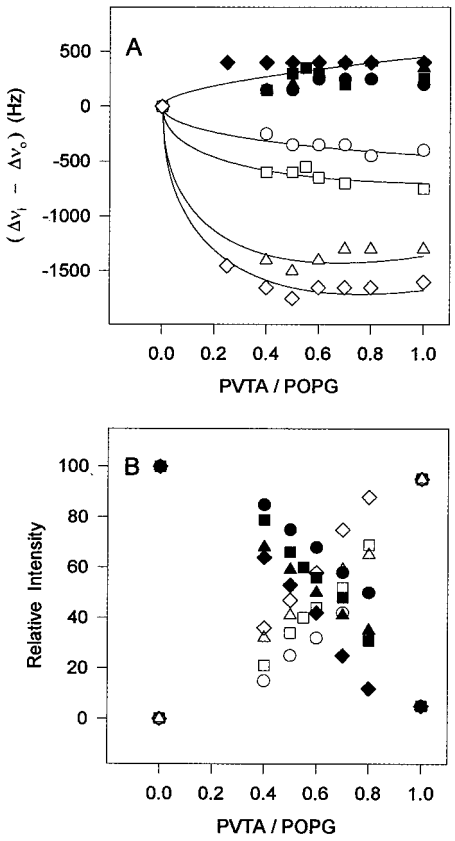

Figure 7. Relative change in the quadrupolar splitting for mixtures of POPG + POPC-β-d_2 (A) and the corresponding intensities of the PVTA-containing and PVTA-free phases as obtained from NMR spectral simulations (B). Circles (●) represent 10/90 POPG/POPC mixtures, squares (■) represent 20/80 mixtures, triangles (▲) represent 30/70 mixtures, and diamonds (◆) represent 40/60 mixtures. Closed symbols represent the PVTA-free phase, while open symbols represent the PVTA-bound phase.

less pronounced, amplification of the decrease in the quadrupolar splitting, relative to the controls, with higher initial POPG content.

The PVTA-bound POPC-β-d_2 component is easily identified from the fact that its intensity increases with added PVTA, as shown in Figure 7B, and this spectral component always displays a quadrupolar splitting less than that of the control, as shown in Figure 7A. In conjunction with the results obtained with POPC-α-d_2, these POPC-β-d_2 measurements confirm that PVTA laterally segregates POPG into a POPG-enriched domain, leaving behind a POPG-depleted domain. In a fashion that is virtually the mirror image of the POPC-α-d_2 results, the decrease in the quadrupolar splitting of POPC-β-d_2 trapped within the PVTA-bound domain, relative to the controls, is again magnified by higher initial POPG levels. For POPC-β-d_2 within the PVTA-free domains, there is a similar, albeit less pronounced, amplification of the decrease in the quadrupolar splitting, relative to the controls, with higher initial POPG content.

These ^{2}H NMR quadrupolar splitting and intensity data indicate that not only is PVTA capable of laterally segregating POPG into POPG-enriched domains but the degree of enrichment increases with higher POPG contents. In effect, the composition and the size of individual PVTA-induced domains appears to depend on the global POPG content of the bilayers. The composition of the domains, and their size, may in fact be extracted from the ^{2}H NMR spectra as follows.

The total populations of zwitterionic (X_z^t) and anionic (X_a^t) lipids present globally in the total lipid bilayer preparation are

conveniently defined in terms of mole fractions according to eq 2.

$$X_z^t = X_a^t = 1 \tag{2}$$

Each of these populations may be subdivided into those which are PVTA-bound (superscript b) and those which are PVTA-free (superscript f), according to eqs 3.

$$X_z^t = X_z^b + X_z^f \tag{3}$$
$$X_a^t = X_a^b + X_a^f$$

The quantities (X_z^b/X_z^t) and (X_z^f/X_z^t) are obtained from the intensities of the two components in the ^{2}H NMR spectra obtained as described above and shown in Figures 6B and 7B.

For cases in which the quadrupolar splitting of deuterated POPC is linearly related to the POPG composition, the quantity X_a^f may be calculated according to eq 4

$$\frac{X_z^f(\Delta\nu^f - \Delta\nu_0)}{(m_i - \Delta\nu^f + \Delta\nu_0)} = X_a^f \tag{4}$$

where $\Delta\nu^f$ is the quadrupolar splitting of deuterated POPC within the PVTA-free domain, $\Delta\nu_0$ is the quadrupolar splitting for 100% POPC, and m_i is the calibration constant for either the α- or β-deutero-labeling position of POPC in the presence of POPG, assuming a linear dependence of the quadrupolar splitting on the mole fraction of POPG. Note that the relevant mole fractions in the calibration eq 1 are terms such as $X_a^f/(X_a^f + X_z^f)$, from which eq 4 above, and eq 5 below, are derived.

For cases in which the second-order term in eq 1 is significant, the quantity X_a^f may be calculated according to eq 5.

$$X_a^f = -X_z^f\left[1 + 2A_i\left(B_i \mp \sqrt{B_i^2 - 4A_i(\Delta\nu^f - \Delta\nu_0)}\right)^{-1}\right]^{-1} \tag{5}$$

Relationships equivalent to eqs 4 and 5 apply for the case of X_a^b.

Note that once X_a^f is determined, one may also calculate the mole fraction of POPG in the PVTA-bound domain by subtraction using eqs 2 and 3. Hence, the compositions of both the PVTA-bound and the PVTA-free domains may be obtained using only the relative intensities of the two ^{2}H NMR spectral components and the quadrupolar splitting of the PVTA-free domain, without specific reference to the quadrupolar splitting of the PVTA-bound domain. Since the PVTA-free domain consists of a binary mixture (POPC + POPG), analysis of its composition from calibration data is straightforward relative to a ternary mixture such as the PVTA-bound domain (POPC + POPG + PVTA). A discussion of this latter case will be deferred for the moment.

The results of applying the above analysis are shown in Figure 8, parts A and B, for POPC-α-d_2 and POPC-β-d_2, respectively. The compositions of the PVTA-free and the PVTA-bound domains are presented in terms of the enrichment, or depletion, relative to the global POPG content present initially in the bilayers. One sees that the PVTA-bound domain is enriched with POPG relative to the initial global composition. Simultaneously, the PVTA-free domain is depleted with respect to POPG. Similar results are obtained for POPC-α-d_2 and POPC-β-d_2. At higher PVTA/ POPG ratios, the composition of the PVTA-bound domain approaches that of the initial global bilayer. This follows from the fact that the entire surface will be covered with polyelectrolyte, so that only the PVTA-bound domain is present.

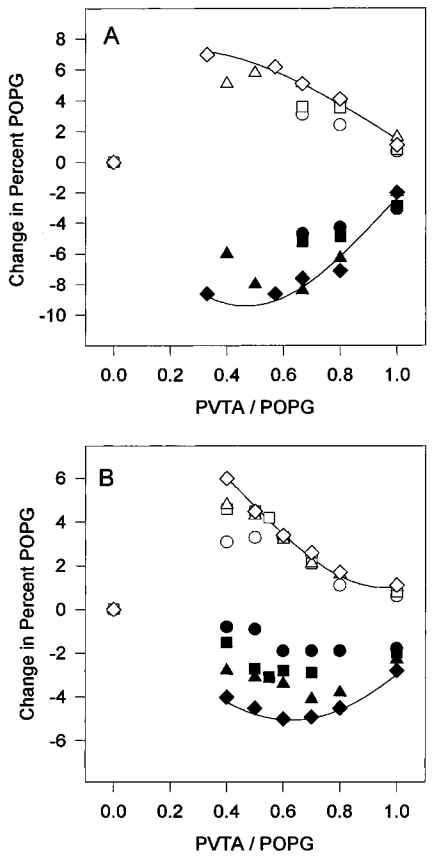

Figure 8. POPG depletion in the PVTA-free phase and enrichment in the PVTA-bound phase as a function of added PVTA for POPG + POPC-α-d_2 mixtures (A) and POPG + POPC-β-d_2 (B). Symbol designations are the same as in Figures 6 and 7.

These data show, in addition, that the degree of enrichment, or depletion, at any one PVTA/POPG ratio is greater for higher initial global POPG contents. For example, at a PVTA/POPG ratio of 0.66, the POPC-α-d_2 data indicate that, for an initial $X_{POPG} = 0.50$, the PVTA-free domains are depleted to $X_{POPG} = 0.43$ while the PVTA-bound domains are enriched to $X_{POPG} = 0.55$. However, at the same PVTA/POPG ratio of 0.66, for an initial $X_{POPG} = 0.20$, the PVTA-free domains are depleted to $X_{POPG} = 0.16$ while the PVTA-bound domains are enriched to $X_{POPG} = 0.23$.

Another useful way of looking at these data is to inquire as to the number of anionic POPG molecules bound per cationic PVTA unit charge. Figure 9 (parts A and B) shows the mole fraction of POPG bound as a function of the PVTA/POPG ratio, as obtained from analysis of the POPC-α-d_2 and POPC-β-d_2 ^{2}H NMR data, respectively. It is evident that there is a 1:1 anion:cation charge ratio within the PVTA-bound domain, regardless of the global POPG content. Put in another fashion, each PVTA polyelectrolyte, being on average some 190 monomer units in length, binds some 190 POPG molecules. This can only occur if the polyelectrolyte is lying flat on the membrane surface, such that every cationic monomer unit of the polyelectrolyte is able to associate with an anionic POPG. Identical conclusions have been reached previously for the case of anionic polyelectrolytes inducing domains in cationic lipid bilayers, provided the amount of added polyelectrolyte anionic charge has not yet exceeded the total lipid bilayer cationic

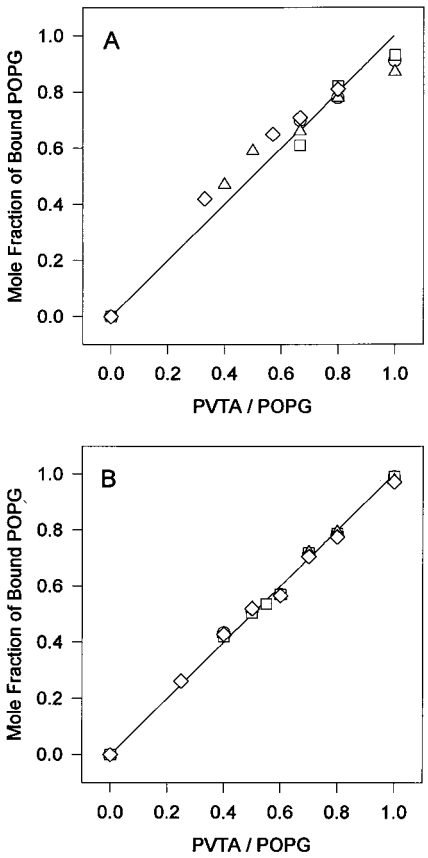

Figure 9. Mole fraction of POPG bound as a function of added PVTA for POPG + POPC-α-d_2 mixtures (A) and POPG + POPC-β-d_2 (B). Symbol designations are the same as in Figures 6 and 7.

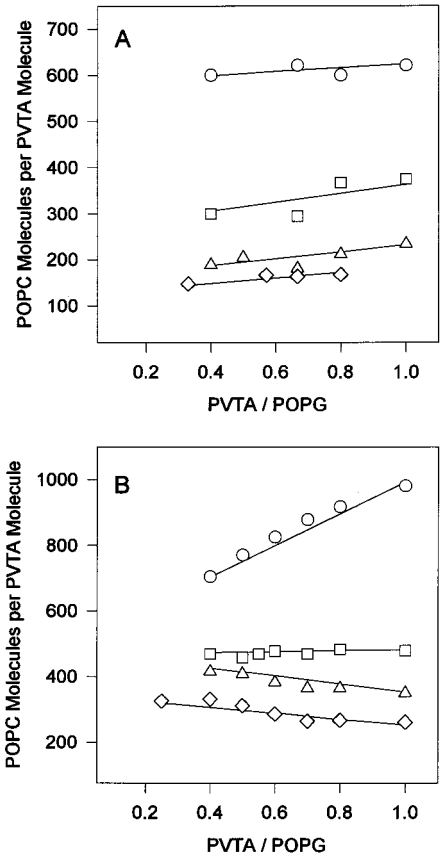

Figure 10. POPC molecules bound per molecule of PVTA as a function of added PVTA for POPG + POPC-α-d_2 mixtures (A) and POPG + POPC-β-d_2 (B). Symbol designations are the same as in Figures 6 and 7.

charge.[11,12] In models of electrostatic binding of peptides and proteins to lipid bilayers it is generally assumed that there is a 1:1 cancellation of lipidic surface charge by peptidyl charges (e.g., ref 10). The data in Figure 9 constitute direct proof of the validity of such an assumption.

If one performs the same type of analysis to obtain the number of zwitterionic POPC molecules bound per cationic PVTA unit charge, as shown in Figure 10, one obtains the rather interesting result that the number of POPC molecules bound per PVTA polyelectrolyte molecule decreases with increasing POPG content of the lipid bilayers.

The surface area occupied by an individual PVTA chain is calculated as the sum of the surface areas occupied by the phospholipids plus that of the polyelectrolyte. POPC and POPG have surface cross sections on the order of 68 Å^2, and one may assume that these values do not change within the domain. The surface cross section of PVTA per monomeric unit is unknown but will depend critically on its degree of penetration into the lipid bilayer. The more important point is that it should be more-or-less constant provided there is no excess of PVTA over POPG. Likewise, given the results in Figure 9, the numbers of POPG per PVTA-defined domain are constant. Thus, the results of Figure 10 indicate that, in effect, the surface area occupied by an individual PVTA chain expands, or contracts, to accommodate more, or less, POPC, depending upon its statistical availability.

A similar finding has been reported for domain formation by the lipid bilayer associating basic peptide cardiotoxin II, which forms 1:1 complexes with anionic lipids such as POPG.[35] When the initial POPG/POPC ratio in the lipid bilayers was increased, the POPC content of the domains formed upon adding cardiotoxin II was found to decrease.

A schematic illustrating this situation for a linear polyelectrolyte is shown in Figure 11, where the cationic polyelectrolyte (black) lying flat on a lipid bilayer membrane surface, as viewed from above, segregates anionic lipids (white) from the midst of the neutral lipid milieu (gray). The polyelectrolyte configuration may be considered to be the result of a random self-avoiding walk on a two-dimensional lattice. The 1:1 cation: anion complex so formed produces a long-lived domain by virtue of electrostatic attraction. Neutral lipids accidentally trapped within the folds of the polyelectrolyte chain cannot exchange quickly with the bulk because the diffusion path length to the domain edge is greatly increased by the tortuosity introduced by the presence of the polyelectrolyte.

Two situations are contrasted in this schematic to summarize our findings. In one case, there is a large mole fraction of anionic lipid overall. This encourages formation of a compact domain entrapping few neutral lipids. In the second case, there is a lower mole fraction of anionic lipid overall. This favors formation of larger domains subsuming many neutral lipids.

In one sense, the neutral lipid composition of the domain may be considered to result from the balance between the unfavorable entropic costs of demixing the anionic lipid and compacting the polyelectrolyte configuration versus the favorable electrostatic attraction between the anionic lipid and the cationic polyelectrolyte. The presence of neutral lipid within the domain simply ameliorates the entropy decrease due to demixing and compacting. In another sense, one may view the neutral lipid composition of the domain as resulting from a process akin to solvent swelling of polymers. The overall neutral anionic lipid−cationic polyelectrolyte complex swells to accommodate neutral lipid, the balance being set by the values

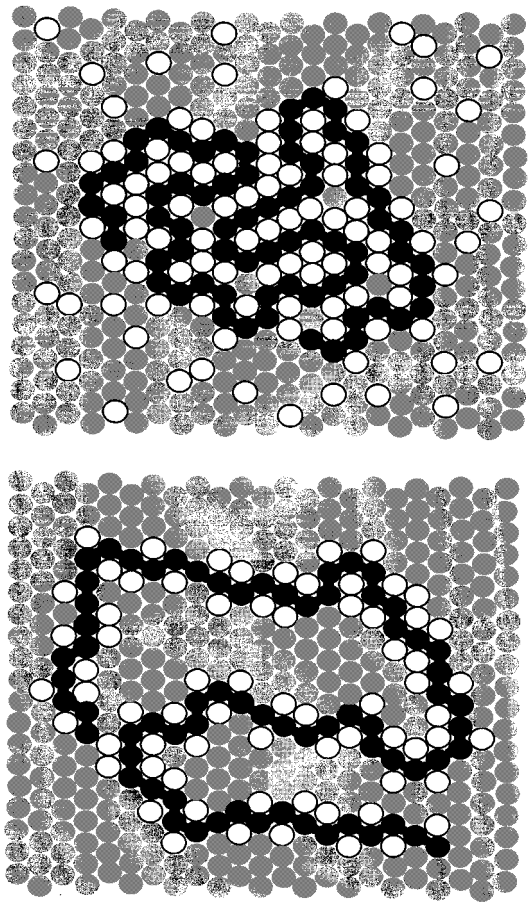

Figure 11. Schematic representation of PVTA (black circles) forming a domain of distinct composition in mixed POPG (open circles) + POPC (closed circles) lipid bilayers.

of interaction parameters between neutral−neutral, complex−neutral, and complex−complex species. Clearly, a better understanding of the thermodynamics of these domains will be needed before further conclusions can be drawn.

If one defines a domain as encompassing that region of the membrane occupied by a single PVTA chain, then we note that these ^{2}H NMR measurements do not provide direct information regarding the extent of aggregation of such individual PVTA chain-defined domains into "super" domains such as those observed via fluorescence spectroscopy.[3] Thus, ^{2}H NMR as used here is limited to providing direct information regarding individual polyelectrolyte chain-defined domain compositions and sizes, and the relative amounts of either domain on a "per polymer chain", rather than an absolute, basis.

Indirectly, however, ^{2}H NMR indicates that aggregation into superdomains probably is occurring. As discussed in detail elsewhere,[11−13] the individual polyelectrolyte chains occupy membrane surface areas too small to permit the observation of separate domains via ^{2}H NMR, assuming that the lipid lateral diffusion coefficients are not radically different in the free versus bound domains. A more direct measure of domain size could be obtained using the ^{2}H two-dimensional exchange NMR procedure introduced by Spiess and co-workers.[36]

^{2}H NMR of POPC in PVTA-Bound Domains. In a ternary mixture of cationic + anionic + zwitterionic species, the observed quadrupolar splitting ($\Delta\nu_\pm$) for choline deuterated POPC is perturbed relative to the value measured for 100% POPC ($\Delta\nu_0$) by an amount that is the sum of the perturbations due to the cationic and anionic species individually in binary mixtures,[37] according to eq 6.

$$(\Delta\nu_\pm - \Delta\nu_0) = (\Delta\nu_- - \Delta\nu_0) + (\Delta\nu_+ - \Delta\nu_0) = m_+X_+ + m_-X_- \quad (6)$$

The quadrupolar splitting in such a ternary mixture may be estimated, therefore, if the relevant calibration constants (m_+ and m_-) are available from calibration experiments in binary mixtures. No such calibration data is available for PVTA since no interaction is observed with 100% POPC lipid bilayers. Hence, to analyze the quadrupolar splittings from the PVTA-bound domains in terms of compositions one is forced to resort to certain assumptions.

Previously, in the case of anionic polyelectrolytes binding to cationic lipid bilayers, it was found that, when it was assumed that the calibration constant for the polyelectrolyte was zero while that for the cationic lipid was unchanged in the polyelectrolyte-bound versus -free domains, the domain compositions obtained from analyzing the quadrupolar splitting of the PVTA-bound POPC were in complete agreement with those obtained by analyzing the PVTA-free POPC.[11,12] In effect, this assumption reduced eq 6 to eq 4. The validity of this approach was rationalized by supposing that the polyelectrolyte was completely masked from exposure to POPC by virtue of its "coating" with electrostatically bound oppositely charged lipid.

In the case of PVTA added to POPG + POPC bilayers, merely assuming that the calibration constant for the polyelectrolyte equals zero fails to bring the lipid composition derived from the quadrupolar splitting of the polyelectrolyte-bound domain into agreement with the composition derived from the quadrupolar splitting of the polyelectrolyte-free domains. Instead, we find it necessary to assume further that the calibration constant for POPG is different in the PVTA-bound versus PVTA-free domain. To estimate this new POPG calibration constant, we plot the quadrupolar splitting from POPC-α-d_2 and POPC-β-d_2 in the PVTA-bound domains for the case of a 1:1 PVTA/POPG charge ratio versus the POPG composition of the PVTA-bound domain derived from the quadrupolar splitting of the corresponding PVTA-free domain. Quadrupolar splitting data for both POPC-α-d_2 and POPC-β-d_2 are available at this PVTA/POPG ratio for all initial POPG contents. Figure 4 shows the results obtained by taking this approach. Apparently, the effective POPG calibration constant within the PVTA-bound domains is significantly larger in magnitude than in the PVTA-free domains, for both POPC-α-d_2 and POPC-β-d_2. The details of the weighting coefficients in the fitted calibration curve are listed in Table 1. When this new calibration curve is applied to the entire set of quadrupolar splittings measured for the PVTA-bound domains, the resulting lipid compositions are in entire agreement with those derived from the quadrupolar splitting for the PVTA-free domains, as shown in Figure 12.

How might one rationalize the apparent changes in the calibration constant for POPG within the PVTA-bound domains? One cannot attribute them to any change in the order parameter of the POPC choline headgroup brought on by exposure to PVTA, since this mechanism should simultaneously increase or decrease both POPC-α-d_2 and POPC-β-d_2 quadrupolar splittings. From a survey of such calibration constants across a series of anionic and cationic species with differing hydrophilic/lipophilic balances, Beschiaschvili and Seelig[38] concluded that the size of the calibration constant correlated with the depth of penetration of the particular species into the membrane surface layer. Species that bound only very superficially tended

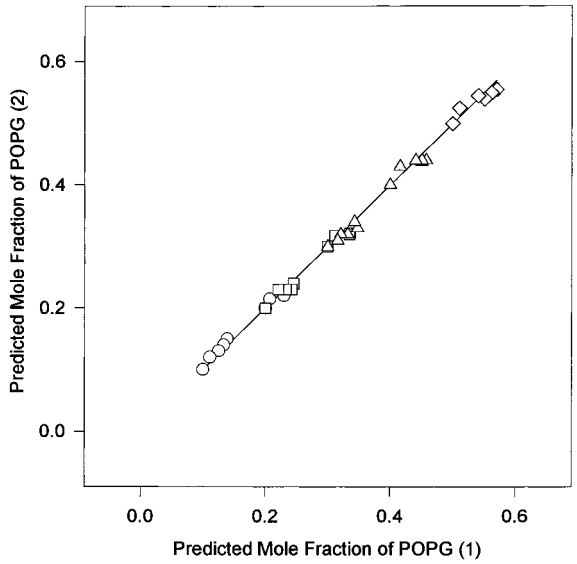

Figure 12. Comparison of the POPG content of the PVTA-bound phase as deduced from the quadrupolar splitting of POPC-α-d_2 and POPC-β-d_2 in the PVTA-free domain (method 1) versus the PVTA-bound domains (method 2). Details are provided in the text.

to yield lower magnitude calibration constants, while more deeply penetrating species yielded higher magnitude constants. For the case at hand, one might suppose, therefore, that the POPG within the PVTA/POPG complex occupies an equilibrium position penetrating more deeply into the membrane proper than that occupied by POPG alone. This would be energetically plausible since the PVTA/POPG complex, consisting of a series of cation:anion salt pairs, is overall neutral. One means of testing this supposition would involve nuclear Overhauser enhancement measurements between POPG and POPC with and without PVTA.

Acknowledgment. This work was supported by a grant from the Natural Sciences and Engineering Research Council (NSERC) of Canada**.**

References and Notes

(1) Thompson, T. E.; Sankaram, M. B.; Biltonen, R. L. *Comments Mol. Cell. Biophys.* **1992**, *8*, 1.

(2) Vaz, W. L. C. *Comments Mol. Cell. Biophys.* **1992**, *8*, 16.

(3) Glaser, M. *Comments Mol. Cell. Biophys.* **1992**, *8*, 37.

(4) Tocanne, J. F. *Comments Mol. Cell. Biophys.* **1992**, *8*, 53.

(5) Edidin, M. *Comments Mol. Cell. Biophys.* **1992**, *8*, 73.

(6) Wolf, D. E. *Comments Mol. Cell. Biophys.* **1992**, *8*, 83.

(7) Jesaitis, A. J. *Comments Mol. Cell. Biophys.* **1992**, *8*, 97.

(8) Buser, C. A.; Kim, J.; McLaughlin, S.; Peitzsch, R. M. *Mol. Membr. Biol.* **1995**, *12*, 69.

(9) McLaughlin, S.; Aderem, A. *TIBS* **1995**, *20*, 272.

(10) Kim, J.; Mosior, M.; Chung, L. A.; Wu, H.; McLaughlin, S. *Biophys. J.* **1991**, *67*, 227.

(11) Mitrakos, P.; Macdonald, P. M. *Biochemistry* **1996**, *35*, 16714.

(12) Mitrakos, P.; Macdonald, P. M. *Biochemistry* **1997**, *36*, 13646.

(13) Crowell, K. J.; Macdonald, P. M. *J. Phys. Chem.* **1997**, *101*, 1105.

(14) Harbison, G. S.; Griffin, R. G. *J. Lipid Res.* **1984**, *25*, 1140.

(15) Aloy, M. M.; Rabout, C. *Bull. Soc. Chim. Fr.* **1913**, *13*, 457.

(16) Aneja, R.; Chada, J. S.; Davies, A. P. *Biochim. Biophys. Acta* **1970**, *218*, 102.

(17) Davis, J. H.; Jeffrey, K. R.; Bloom, M.; Valic, M. I.; Higgs, T. P. *Chem. Phys. Lett.* **1976**, *42*, 390.

(18) Rance, M.; Byrd, R. A. *J. Magn. Reson.* **1983**, *52*, 22.

(19) Alderman, D. W.; Solum, M. S.; Grant, D. M. *J. Chem. Phys.* **1986**, *84*, 3717.

(20) Seelig, J. *Q. Rev. Biophys.* **1977**, *10*, 353.

(21) Seelig, J.; Seelig, A. *Q. Rev. Biophys.* **1980**, *13*, 19.

(22) Seelig, J.; Macdonald, P. M.; Scherer, P. G. *Biochemistry* **1987**, *26*, 7535.

(23) Macdonald, P. M. *Acc. Chem. Res.* **1997**, *30*, 196.

(24) Sternin, E.; Bloom, M.; MacKay, A. L. *J. Magn. Reson.* **1983**, *55*, 274.

(25) Marassi, F. M.; Macdonald, P. M. *Biochemistry* **1991**, *30*, 10558.

(26) Mitrakos, P.; Macdonald, P. M. *Biochim. Biophys. Acta* **1998**, *1374*, 21.

(27) Köchy, T.; Bayerl, T. M. *Phys. Rev. E* **1993**, *47*, 2109.

(28) Macquaire, F.; Bloom, M. *Phys. Rev. E* **1995**, *51*, 4735.

(29) Dolainsky, C.; Unger, M.; Bloom, M.;& Bayerl, T. *Phys. Rev. E* **1995**, *51*, 4743.

(30) Seelig, J. *Biochim. Biophys. Acta* **1978**, *515*, 105.

(31) Cullis, P. R.; de Kruijff, B. *Biochim. Biophys. Acta* **1979**, *559*, 399.

(32) Wohlgemuth, R.; Waespe-Šarčeviĉ, N.; Seelig, J. *Biochemistry* **1980**, *34*, 1500.

(33) Tamm, L.; Seelig, J. *Biochemistry* **1983**, *22*, 1474.

(34) Scherer, P. G.; Seelig, J. *Biochemistry* **1989**, *31*, 1092.

(35) Carbone, M. A.; Macdonald, P. M. *Biochemistry* **1996**, *35*, 3368.

(36) Schmidt, C.; Blümich, B.; Spiess, H. W. *J. Magn. Reson.* **1988**, *79*, 269.

(37) Marassi, F. M.; Macdonald, P. M. *Biochemistry* **1992**, *31*, 10031.

(38) Beschiaschvili, G.; Seelig, J. *Biochemistry* **1990**, *29*, 52.